# An *in vivo* pharmacological study of single group Ia fibre contacts with motoneurones in the cat spinal cord

Bruce Walmsley and Philip S. Bolton

*The Neuroscience Group, University of Newcastle, University Drive, Callaghan, NSW 2308, Australia*

1. Direct experimental evidence was obtained on the spatial distribution of active synaptic contacts from single Ia muscle afferents on the dendrites of lumbosacral motoneurones in anaesthetized cats.

2. An extracellular micropipette was used to pressure eject the AMPA/kainate receptor antagonists 6-cyano-7-nitroquinoxaline-2,3-dione (CNQX) or 2,3-dihydroxy-6-nitro-7-sulphamoyl-benzo(F)quinoxaline (NBQX) in close proximity to the intracellular recording site, in order to create an extracellular concentration gradient of the antagonist. The effect of antagonist ejection on the time course and amplitude of excitatory postsynaptic potentials (EPSPs) evoked in motoneurones by impulses in single group Ia fibres was examined.

3. Pressure ejection of NBQX resulted in a complete block of the monosynaptic group Ia EPSP in two cells, and a significant reduction to 23–57% of control EPSP peak amplitudes in a further six cells (mean, 27%; $n = 8$). These effects were not associated with changes in membrane potential or membrane time constant.

4. The reduction in amplitude of these single group Ia fibre EPSPs following ejection of NBQX was usually accompanied by a pronounced slowing in the time course of the EPSPs. On average, the EPSP rise times and half-widths were increased by 269 and 37%, respectively. This is most probably due to a considerable spatial spread of the synaptic contacts along the dendrites of motoneurones, with the most proximal synaptic contacts (producing the briefest synaptic potentials) subjected to a greater reduction in amplitude due to a higher local antagonist concentration.

5. An equivalent dendritic cable model of the motoneurone was used to interpret the observed changes in the time course of single fibre EPSPs. The time course of control single fibre EPSPs examined in the present study could be well matched using the cable model and assuming a single location for synaptic input. The observation of a slowed EPSP time course following antagonist ejection indicated that this assumption was not correct and that there was in fact considerable spatial spread in the synaptic contacts arising from these single afferent fibres. These results provide direct evidence that spatial spread of synaptic input may not be detected using the time course of a synaptic potential in conjunction with a neuronal cable model of the postsynaptic cell.

Interpretation of the results of previous *in vivo* electrophysiological studies of the monosynaptic connection between group Ia afferent fibres and spinal motoneurones has been complicated by the spatial (electrotonic) spread of synaptic contacts over the soma and large dendritic trees of these neurones (Walmsley & Stuklis, 1989). In addition, the inability of locally applied pharmacological agents to reach all activated synapses has led to equivocal results regarding the nature of the postsynaptic receptors at this connection (Flatman, Durand, Engberg & Lambert, 1987). These results have been further complicated by the use of composite (multifibre) EPSPs. The time course of a composite EPSP is affected by dispersion in the arrival times of action potentials at synaptic contacts arising from different afferent fibres (due to different conduction velocities), and the likelihood of contaminating polysynaptic EPSPs and IPSPs due to convergent multifibre inputs to interneurones which project to motoneurones in the spinal cord. Until the present study, there have been no single fibre studies using pharmacological antagonists of Ia excitatory postsynaptic potentials (EPSPs) evoked in cat spinal motoneurones.

Many previous electrophysiological studies have used the time course of single Ia fibre EPSPs in conjunction with an equivalent cable model of the motoneurone to calculate an electrotonic location for the site of generation of the single fibre EPSPs (e.g. Rall, Burke, Smith, Nelson & Frank, 1967; Jack, Miller, Porter & Redman, 1971; Iansek & Redman, 1973*b*; Rall, Burke, Holmes, Jack, Redman & Segev, 1992). Although these studies assumed that the synaptic contacts arising from a single fibre were made over a very restricted region of the dendritic tree, anatomical evidence indicates that this assumption is not generally justified (Brown & Fyffe, 1978; Burke, Walmsley & Hodgson, 1979; Glenn, Burke, Fleshman & Lev-Tov, 1982). However, quantal analysis of single Ia fibre EPSPs has raised the further possibility that only some of these contacts are active, and the anatomical evidence is therefore not conclusive (Redman & Walmsley, 1983; Redman, 1990; Walmsley, 1992). In addition, it has been shown in a previous modelling study that it is generally not possible to use the time course of the EPSP in conjunction with a neuronal cable model to detect spatial dispersion of synaptic input (Walmsley & Stuklis, 1989).

The present experiments were therefore designed to obtain the first direct experimental evidence on the spatial dispersion of active synapses at the connection between single Ia fibres and motoneurones in the cat spinal cord *in vivo*.

## METHODS

Experiments were performed on twenty-one cats weighing 1·5–3·0 kg. The cats were anaesthetized with sodium pentobarbitone (35 mg $kg^{-1}$ I.P.) and maintained with supplementary doses (5 mg $kg^{-1}$ I.V.). All animals respired naturally. At the end of the experiment each animal was killed by an overdose of sodium pentobarbitone (120 mg $kg^{-1}$ I.V.)

Muscle nerves in the left hindlimb were exposed, cut and placed on bipolar stimulating electrodes. These included the nerves to the posterior biceps, semitendinosus, medial gastrocnemius, lateral gastrocnemius, soleus and plantaris. The lumbosacral cord was exposed by laminectomy from L2 to L7. Methods for obtaining and recording single fibre EPSPs were identical with those outlined in previous studies (see Tracey & Walmsley, 1984). Briefly, a dorsal root filament was selected (using bipolar electrical recording) which contained only a single group I fibre from each of the dissected hindlimb nerves, or as many of the nerves as possible. Following selection of a suitable dorsal root filament, all other dorsal roots were cut from L3 to S2, so that the selected filament contained the only input to the spinal cord from the dissected hindlimb nerves. Single fibre EPSPs were evoked in motoneurones by electrical stimulation of the appropriate hindlimb nerve, at a frequency of 3–6 pulses $s^{-1}$. Several initial experiments were performed using multifibre EPSPs (all dorsal roots intact), in order to develop the double-microelectrode technique and to enable comparison with previous pharmacological studies using multifibre EPSPs.

Electrotonic measurements of motoneurones were obtained using the voltage response to a brief intracellular current pulse (usually 10 nA amplitude, 200 $\mu$s duration, Iansek & Redman, 1973*a*). As pointed out by Iansek & Redman (1973*a*), a major advantage of the brief current pulse technique over the use of long-duration current pulses is that the contribution of the voltage drop across the electrode resistance is avoided in the case of the brief current pulse response. In order to compare the present results with previous experiments, the electrotonic length of an equivalent dendritic cable ($L$) and the dendritic-to-somatic conductance ratio were calculated for selected cells using the methods described by Jack & Redman (1971). This method is based on a comparison of the time course of the initial, steep decay phase and the final decay phase of the voltage response of the cell to the brief intracellular current pulse. The neuronal cable model was then used to interpret the time course of the single fibre EPSPs recorded in the cell by calculating the time course of voltage transients generated by current injection at various electrotonic locations using the methods described in Jack & Redman (1971) and Walmsley & Stuklis (1989).

### Spatial pharmacological block of synaptic potentials

A micropipette (tip diameter, approximately 1 $\mu$m) was glued to the intracellular pipette 30–80 $\mu$m from the tip, so that pharmacological agents could be ejected extracellularly in close proximity to the intracellular recording electrode. The AMPA/kainate antagonists CNQX (2 mM, Tocris Neuramin, Bristol, UK), and NBQX (1 mM, Novo-Nordisk, Copenhagen, Denmark) dissolved in 0·9% (w/v) NaCl were ejected using pressure from the extracellular pipette. Pressure was applied in pulses by hand using a 5 ml disposable syringe attached by a flexible tube to the pressure port of the electrode holder.

The localized extracellular ejection of a highly concentrated antagonist solution creates a concentration gradient in the extracellular fluid. Such a gradient results in a concentration of antagonist which is greatest at synapses closest to the electrode. Due to the electrotonic properties of the dendritic tree, proximal synaptic inputs contribute synaptic potentials with a much briefer time course than more distal synapses. Therefore, following ejection of the antagonist, a progressive block from proximal to distal synapses should be detected as a progressive slowing of the time course (in particular the rise time) of the evoked single fibre EPSP, thus indicating spatial dispersion of active synapses arising from the single fibre. On the other hand, if all synapses arising from a single fibre were at the same electrotonic distance from the recording electrode, then the time course of the single fibre EPSP should remain the same, and simply decrease in amplitude during the progressive block. (The latter argument also applies if the synapses are physically at different distances from the electrode but, due to the dendritic geometry, are at the same electrotonic distance.)

The time course of single fibre EPSPs and the membrane properties of the postsynaptic cell were monitored before and after ejection of CNQX or NBQX from the extracellular electrode. Sequential trials of 200–500 EPSPs were averaged and stored on computer disk. Several averaged control EPSPs were usually recorded to examine the reproducibility of the EPSP amplitude and time course parameters in each cell. The rise time of an EPSP was calculated as the time from 10 to 90% of the peak amplitude on the rising phase. The half-width of an EPSP was calculated as the time from 50% of the peak amplitude on the rising phase to 50% of the peak amplitude on the decay phase. The difference between sequential control values of peak amplitude, rise time and half-width provided a measure of the accuracy and

reproducibility of these parameters. Changes in these parameters following antagonist ejection were assessed by comparison with the reproducibility of control values.

## RESULTS

Intracellular recordings were obtained from motoneurones in the spinal cords of twenty-one cats. Cells were only selected for further analysis if the membrane potentials were stable and more negative than −60 mV. Considerable difficulty was experienced in obtaining the joint requirements of a cell with a demonstrated single Ia fibre input, adequate ejection via the extracellular micropipette (which often became blocked), and an absolutely stable penetration for the duration of the recording period. These requirements were achieved in a total of nine cells.

### Block of composite EPSPs by CNQX and NBQX

The previous intracellular pharmacological study of composite Ia EPSPs by Flatman *et al.* (1987) demonstrated a reduction of the composite EPSP with γ-D-glutamyl-aminomethylsulphonate (GAMS) and *cis*-2,3-piperidine-dicarboxylate (PDA; see also Davies & Watkins, 1983, 1985). We have repeated these experiments using the potent AMPA/kainate antagonists, CNQX and NBQX (Honoré *et al.* 1988; Watkins, Krogsgaard & Honoré, 1990). Acceptable results were obtained in three cells. The results obtained from one experiment are illustrated in Fig. 1. The control EPSP peak amplitude of 0·48 mV varied by less than 1% in sequential averages of 200 trials. Pressure ejection of CNQX produced a decrease in the amplitude of the composite EPSP to 56% of the control peak amplitude. There was a marked slowing of the rising phase of the composite EPSP, and this is more clearly observed on the normalized (to peak amplitude) EPSP traces shown in Fig. 1*B*. The rise time (0·81 ms) and half-width (8·8 ms) of the control EPSP were slowed by CNQX ejection to 1·2 and 10·9 ms, respectively. However, no significant difference was observed between the time constant of the final decay phase of the control EPSP (10·5 ms) and the time constant of the EPSP reduced by CNQX ejection (10·7 ms). No detectable change was observed in the amplitude of the antidromic action potential (95 mV), nor in the resting membrane potential (−70 mV). The recurrent Renshaw IPSP, evoked by ventral root stimulation, was also unchanged by the CNQX ejection. These results indicate that there was no detectable non-specific action of the pressure injection procedure used in these experiments.

Similar results were obtained for composite EPSPs in a further two cells using CNQX or NBQX ejection, with decreases in peak amplitude to 31 and 46% of the respective control EPSP peak amplitudes. The composite EPSPs recorded in all three cells exhibited slower time courses during antagonist ejection. This result is very similar to that obtained by Flatman *et al.* (1987) on composite EPSPs, for which the most likely explanation is that the antagonist is not able to reach distal synapses in an adequate concentration. The interpretation is complicated by the use of multifibre inputs with different conduction delays, and the possibility of polysynaptic excitatory contamination (see Discussion).

### Effect of NBQX on single group Ia fibre EPSPs

Acceptable results were obtained on the effect of NBQX for a total of eight single Ia fibre EPSPs.

Figure 2*A* and *B* illustrates the effect of pressure ejection of NBQX on two single Ia fibre EPSPs recorded in different motoneurones, with control peak amplitudes of 0·112 and 0·133 mV, respectively. Sequential control EPSP peak amplitudes, averaged over 200 trials, were within 4% for both EPSPs. Both EPSPs exhibited a rapid rising phase, indicating that a component of the synaptic input was generated electrotonically close to the recording site. The rise times of the EPSPs illustrated in Fig. 2*A* and *B* are 0·27 and 0·19 ms, respectively (reproducible within 2 and 7%). The EPSP in Fig. 2*A* was rapidly and completely blocked by pressure ejection of NBQX. The EPSP

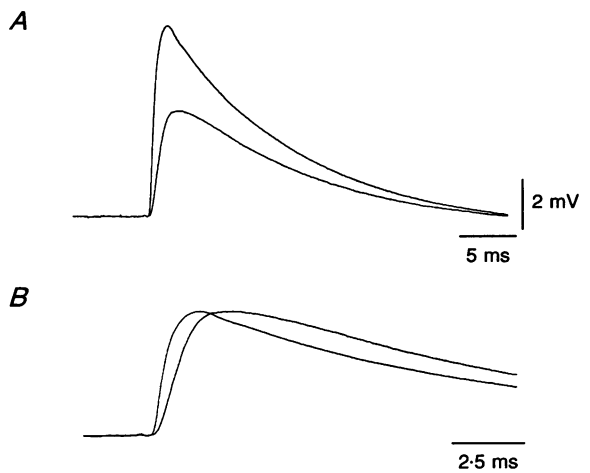


**Figure 1. The effect of localized extracellular CNQX ejection on a composite group I EPSP recorded in a motoneurone**
*A*, the control EPSP (*A*, top trace) was reduced in amplitude by ejection of CNQX (1 mM) from an extracellular electrode (*A*, lower trace). Each EPSP trace represents the average of 200 trials. *B*, the difference in time course of the control EPSP and the reduced EPSP (slower rising phase), normalized to the same peak amplitude (arbitrary scale).

illustrated in Fig. 2*B* was not completely blocked by NBQX, although the residual EPSP exhibited a much slower rising phase than the control EPSP.

Complete block of a monosynaptic single Ia fibre EPSP with NBQX was observed in one other experiment, illustrated in Fig. 2*C*. The control EPSP exhibited a rapid rising phase, although the decay phase was complicated by a polysynaptic EPSP which was delayed by approximately 1 ms (and which is most clearly observed in the lower trace showing a complete block of the monosynaptic EPSP). Analysis of sequential averages (500 trials each) of the control EPSP revealed an average peak amplitude of 0·092 mV and a rise time of 0·27 ms (reproducible within 2 and 7%, respectively, in sequential averages). Following NBQX ejection, the monosynaptic Ia EPSP was very rapidly blocked, and recovered over a period of approximately 6 min back to 90% of the control peak amplitude. During the recovery period sequential averages (400–800 trials) were obtained, and three of these averages are illustrated between the control and blocked EPSP traces in Fig. 2*C*. In contrast to the marked slowing of the rising phase of the EPSP illustrated in Fig. 2*B*, the average rise time of the reduced EPSPs (0·24 ms) illustrated in Fig. 2*C* was very similar to the control value (0·27 ms). The most likely explanation for this result is that the synaptic contacts generating this EPSP are all close to or at the soma of the cell. This result also indicates that there is not an intrinsically slow component to the synaptic current (such as an NMDA receptor-mediated current; see Discussion).

Figures 3*A* and *C* and 3*B* and *D* illustrate two further single Ia fibre EPSPs recorded in different motoneurones, prior to and following pressure ejection of NBQX. NBQX produced a significant reduction in the amplitude of both EPSPs. The EPSPs in Fig. 3*A* and *B* were reduced to 39 and 35% of their respective control peak amplitudes (0·151 and 0·100 mV). The normalized (to peak amplitude) time courses of both EPSPs are illustrated in Fig. 3*C* and *D*. The NBQX block clearly resulted in a pronounced slowing of the rising phase of both EPSPs.

## Equivalent cable model and the time course of single Ia fibre EPSPs

Figure 4*A* illustrates the reduction in amplitude of a single Ia fibre EPSP, following ejection of NBQX. (The control EPSP peak amplitude of 0·476 mV was consistent to within 1% in sequential averages of 200 trials.) This reduction in amplitude was accompanied by a pronounced slowing of the rising phase, which is more evident in the plot of normalized amplitudes, shown in Fig. 4*B*. The rise time more than doubled from 0·70 ms for the control EPSP to 1·58 ms for the reduced EPSP. (Sequential control rise time values were within 3%.) A semilogarithmic plot of the control and reduced EPSPs is illustrated in Fig. 4*C*. A linear regression fit to the decay phase of the EPSPs revealed that the time constant of decay was the same for the control EPSP and for the reduced EPSP, both being equal to 10·1 ms. This indicates that there was no change in the membrane time constant following ejection of NBQX. The voltage response to a brief intracellular current pulse (amplitude, 20 nA; duration, 200 $\mu$s) was also recorded in this cell (Fig. 4*D*), and the time constant of the final decay (Fig. 4*D*, plot *a*) closely matched that of the EPSPs (10·9 ms).

The current pulse response for the cell illustrated in Fig. 4 was further analysed using the method of Jack & Redman (1971), to provide an equivalent cable model of the cell. Figure 4*D* illustrates linear regression fits to the final decay (representing the membrane time constant, curve *a*) and to the initial, rapid decay (curve *b*, obtained by

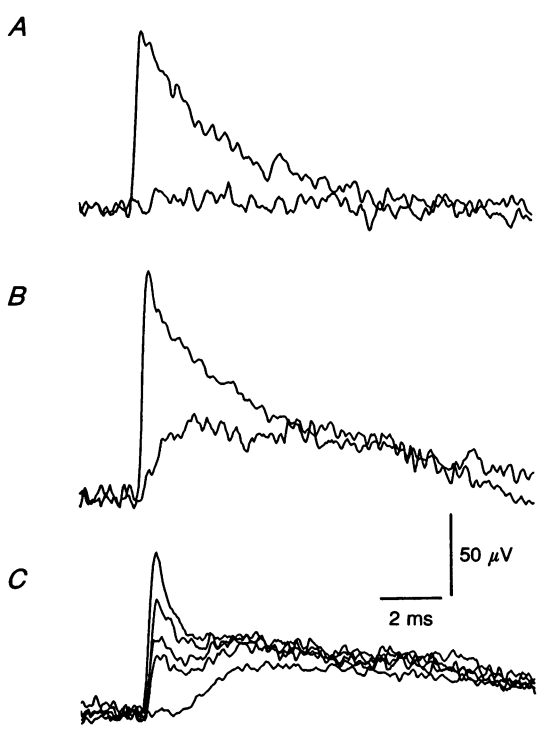


**Figure 2. NBQX reduction of single Ia fibre EPSPs**
Reduction in amplitude of three single fibre Ia EPSPs recorded in different motoneurones following ejection of NBQX (2 mM) from an extracellular electrode. Traces represent averages of 200 trials in *A* and 500 trials in *B*. *C*, five superimposed averages of 500 trials each, illustrating the control EPSP (uppermost trace), complete block of the monosynaptic component of the EPSP (lowermost trace), and three intermediate averages (see text).

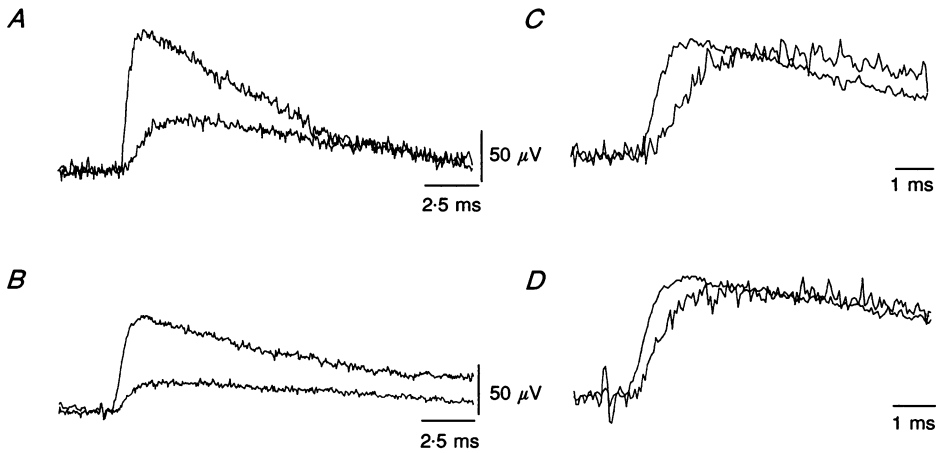


**Figure 3. Localized ejection of NBQX slows the time course of single Ia fibre EPSPs**
Reduction in amplitude of two single Ia fibre EPSPs recorded in different motoneurones (*A* and *B*), following ejection of NBQX (2 mM) from an extracellular microelectrode. The normalized time courses (to peak amplitude) of the control and partially blocked EPSPs are illustrated in *C* and *D* (arbitrary amplitude scales) corresponding to *A* and *B*, respectively. Traces represent averages of 400 trials in *A* and 500 trials in *B*.

subtracting the regression fit to the final decay from the current pulse response). As described by Jack & Redman (1971), comparison of these initial and final decay phases can be used to reveal the electrotonic properties of the cell. This analysis produced a lumped resistance and capacitance soma, finite length dendritic cable model of this cell with an equivalent cable length ($L$) of 1·0 space constants, and a dendritic to somatic conductance ratio of 25. This cable model was used to examine the time courses of the control and reduced EPSPs recorded in this cell, using the same procedure performed in previous studies of single fibre EPSPs (Iansek & Redman, 1973*b*).

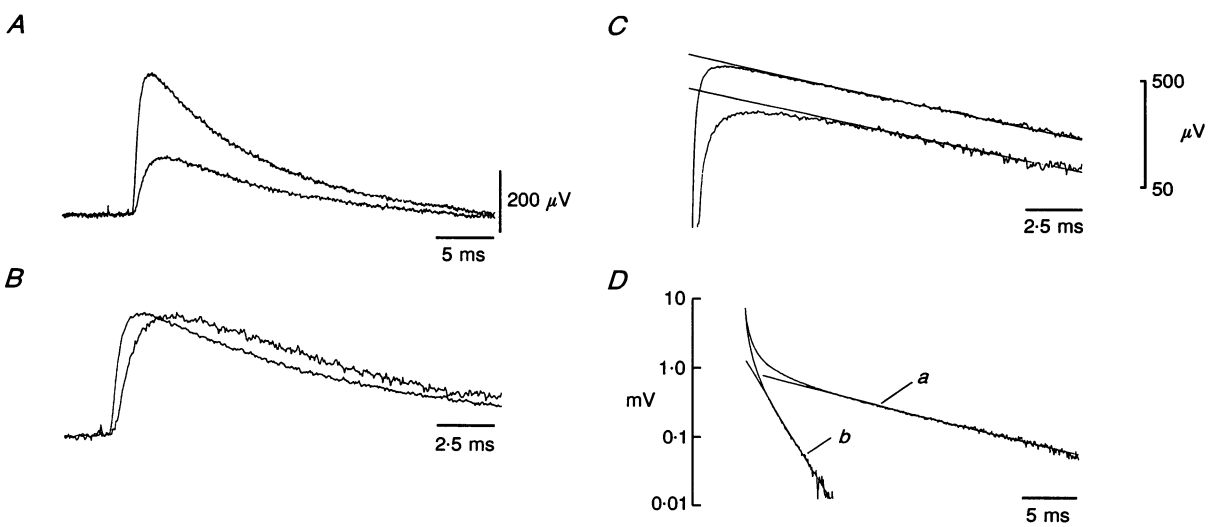


**Figure 4. NBQX reduction and slowing in time course of a single Ia fibre EPSP is not associated with changes in cell membrane time constant**
*A*, control (upper) and reduced (lower) single Ia fibre EPSP using extracellular ejection of NBQX (2 mM). Each EPSP trace represents the average of 200 trials. *B*, the normalized (to peak amplitude) time courses of the EPSPs illustrated in *A*. *C* illustrates these EPSPs plotted on logarithmic amplitude scale (straight lines superimposed on these curves represent linear regression fits to the decay phase of these EPSPs). *D*, the voltage response (average response of 400 trials, logarithmic amplitude scale) to a brief intracellular current pulse (20 nA, 200 μs) in this cell (curve *a*). *D*, curve *b*, the difference between the linear regression fit to the final decay phase and the complete voltage response (curve *a*). The straight line in curve *b* represents a linear regression fit to the final decay phase of this difference curve.

Figure 5A illustrates the control single fibre EPSP (curve *a*). The rise time and half-width of this EPSP divided by the membrane time constant (normalized rise time and normalized half-width) are 0·07 and 0·83, respectively. These shape indices were closely matched by current injection, $I(T) = T\exp(-\alpha T)$, at a single point on the cable, $X = 0{\cdot}5$ space constants from the soma, determined iteratively using the cable model. The normalized rise time and normalized half-width of the generated transient are 0·07 and 0·85 at the model soma. The complete time course of this transient is illustrated (smooth curve) overlying the control EPSP (curve *a*) in

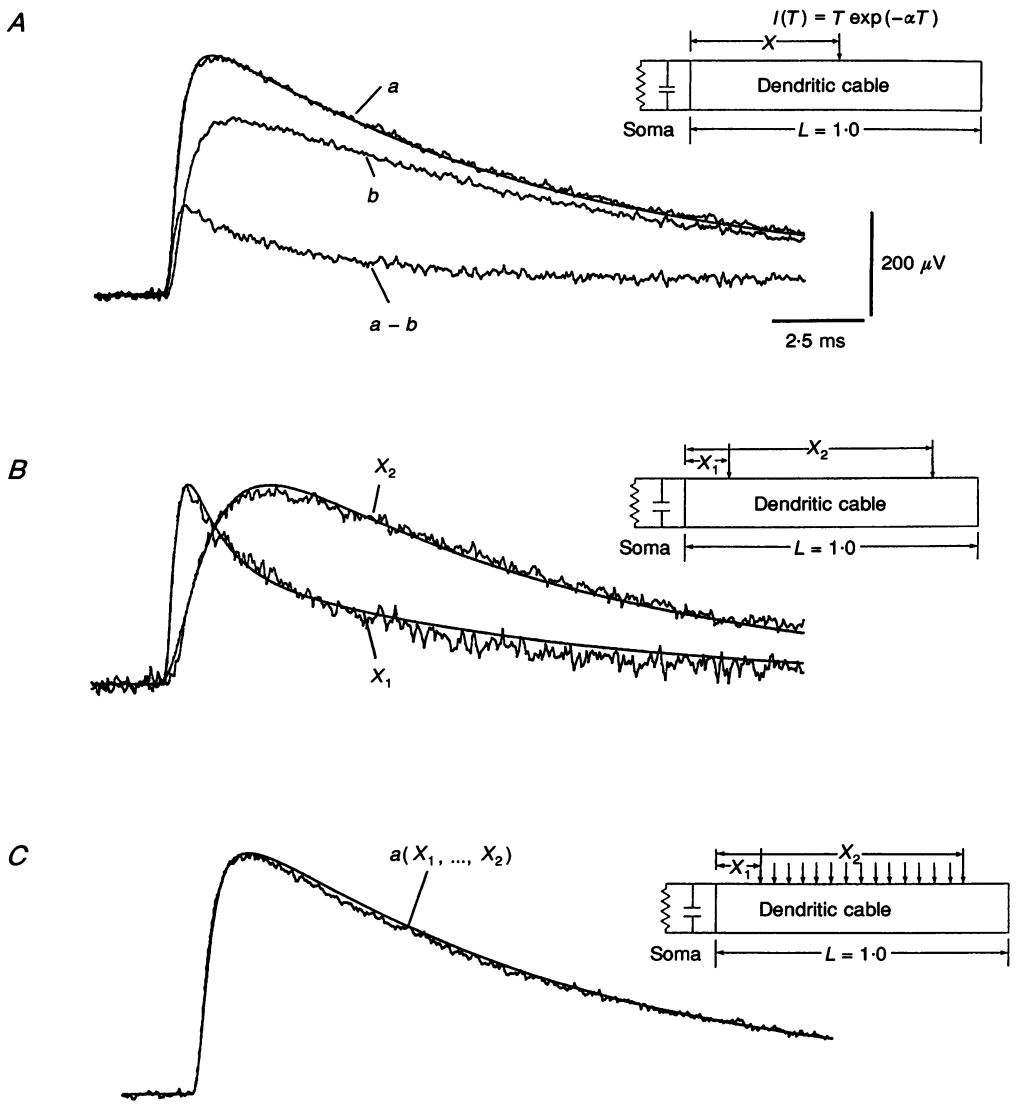


**Figure 5. The use of a cable model of the motoneurone to interpret changes in the time course of a single Ia fibre EPSP**

*A*, curve *a*, the same control EPSP shown in Fig. 4; curve *b*, the reduced EPSP immediately following extracellular ejection of NBQX; curve *a* − *b*, the difference between the control EPSP (curve *a*) and the reduced EPSP (curve *b*). The cable model of the cell (illustrated at the right of *A*) was used to generate a fit to the time course of the control EPSP, assuming a single location for synaptic input, and this fit is shown as the smooth curve overlying the control EPSP. *B*, the normalized (to peak amplitude) time courses of this difference component ($X_1$) and the EPSP after NBQX had its maximal effect ($X_2$, also illustrated in Fig. 4*A*). The smooth curves overlying these EPSPs represent the fits obtained using the cable model and assuming a single synaptic input location for each EPSP ($X_1$ and $X_2$, shown at the right of this figure). *C* again illustrates the control EPSP time course. The smooth curve ($X_1$, ..., $X_2$) overlying the control EPSP represents the fit generated using the cable model and evenly distributing the synaptic input between $X_1$ and $X_2$ (as shown at the right of the figure).

Fig. 5*A*, and it is apparent that the EPSP time course can be very well matched by assuming a restricted location for the synaptic current. Curve *b* in Fig. 5*A* illustrates the time course of the EPSP 4 min after pressure ejection of NBQX. This reduced EPSP was subtracted from the control EPSP (curve *a*) to produce the curve ($a - b$) in Fig. 5*A*. This curve represents the time course of the component of the EPSP which was initially blocked during the application of the NBQX, and is replotted, normalized to peak amplitude, in Fig. 5*B* (curve $X_1$). The EPSP remaining after the NBQX had its maximal effect (illustrated in Fig. 4*A*), is also replotted in Fig. 5*B* (curve $X_2$). Thus, curves $X_1$ and $X_2$ demonstrate the most rapid ($X_1$) and the slowest ($X_2$) components of the single Ia fibre EPSP which could be revealed in this cell. The equivalent cable model was used to analyse these components, assuming a restricted location for the input current. The normalized rise time (0·036) and normalized half-width (0·30) of the fast component ($X_1$) were well matched (0·036 and 0·29, respectively) by a current injection at $X_1 = 0{\cdot}23$ space constants from the model soma. The normalized rise time (0·16) and normalized half-width (0·98) of the slow residual EPSP were matched (0·16 and 1·0, respectively) with a current location at $X_2 = 0{\cdot}85$ space constants from the soma.

The anatomical distribution of synaptic inputs to the dendritic tree of the motoneurone at this connection is, of course, unknown. However, it is apparent from the results illustrated in Fig. 5*B* that the synaptic input is distributed widely over the dendritic tree in terms of electrotonic distance. Clearly, the assumption of a restricted location for synaptic input (Fig. 5*A*) was incorrect, despite an excellent match to the EPSP time course under this assumption. Figure 5*C* illustrates that, if the synaptic input is distributed evenly from the closest ($X_1 = 0{\cdot}2$ space constants) to the most distal ($X_2 = 0{\cdot}85$) estimates obtained from the analysis of Fig. 5*B*, that a good match of the resultant somatic transient (normalized rise time = 0·07, normalized half-width = 0·88) can be obtained to the control EPSP (normalized rise time = 0·07, normalized half-width = 0·83). This direct experimental demonstration supports the results of our previous theoretical study, that the time course of an EPSP cannot generally be used to confirm a restricted location for synaptic input.

In a further experiment (Fig. 6), we were able to record two different single Ia fibre EPSPs in the same motoneurone. These EPSPs exhibited similar peak amplitudes of 131 and 124 $\mu$V for the control EPSPs illustrated in Fig. 6*A* and *B*, respectively, which were consistent to within 3% in sequential averages of 500 trials. Despite having similar peak amplitudes, these EPSPs demonstrated quite different time courses, with the EPSP in Fig. 6*B* having a much slower rising phase and initial decay (rise time = 1·27 ms, half-width = 10·2 ms) than the brief EPSP illustrated in Fig. 6*A* (rise time = 0·40 ms, half-width = 4·53 ms).

The voltage response to a brief intracellular current pulse (10 nA, 200 $\mu$s) was recorded in this cell, and subsequently analysed to construct an equivalent cable model of the motoneurone. The equivalent cable length for the cell $L$ was 1·3 space constants, and the dendritic to somatic conductance ratio was 8·6. Using this cable model, a match was found to the time course of the single fibre EPSPs using the shape indices (normalized rise time and normalized half-width). The shape indices of the EPSP illustrated in Fig. 6*A* (normalized rise time = 0·03, normalized half-width = 0·35) were matched (normalized rise time = 0·03, normalized half-width = 0·35) with a single location input on the cable model at an electrotonic distance from the soma $X = 0{\cdot}28$ space constants. The time course of the transient generated using the cable model is illustrated by the smooth curve in Fig. 6*A*, superimposed on the averaged EPSP time course. A similar analysis was performed for the single fibre EPSP illustrated in Fig. 6*B*. This EPSP exhibited a normalized rise time = 0·10 and normalized half-width = 0·78, and these parameters were also well matched (normalized rise time = 0·10, normalized half-width = 0·79) using a single location current input to the equivalent cable model at $X = 0{\cdot}54$ space constants from the model soma (smooth curve in Fig. 6*B*). The effect of ejection of NBQX on both of these single fibre EPSPs is illustrated in Fig. 6*A* and *B*. A significant reduction was

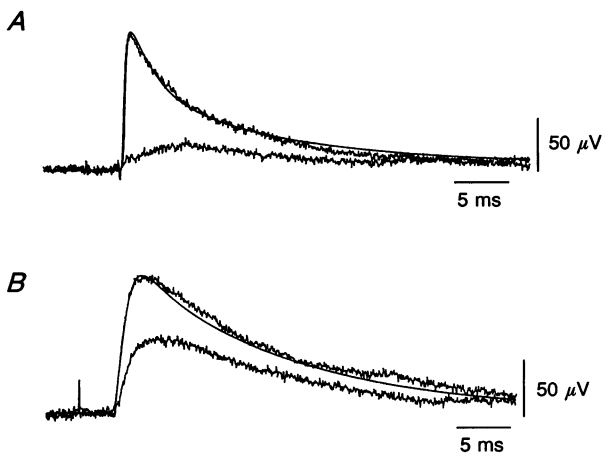


**Figure 6. Differential effect of localized NBQX ejection on two different single Ia fibre EPSPs evoked in the same motoneurone**
*A* and *B* illustrate two different single Ia fibre EPSPs recorded simultaneously in the same motoneurone before (upper records in *A* and *B*) and following (lower records in *A* and *B*) ejection of NBQX (2 mM) from an extracellular electrode. Each EPSP trace represents the average of 500 trials. The smooth curves in *A* and *B* represent fits to the control EPSPs obtained using a cable model for this cell (see text for further explanation).

observed for both EPSPs, although the reduction was much greater for the brief EPSP in Fig. 6*A* than the slower EPSP shown in Fig. 6*B*, these EPSPs being reduced to 22 and 57% of their respective control peak amplitudes. This observation is consistent with a more proximal location (on average) for the synaptic input generating the brief EPSP than for the slower EPSP. In this case, it was not possible to obtain a match to the time courses of the partially blocked EPSPs using the simple equivalent cable model. However, the time courses of both EPSPs exhibited a significant slowing, particularly the rising phase, an effect which was again more obvious for the EPSP in Fig. 6*A* than the EPSP shown in Fig. 6*B*. It is clear that it was not valid to model the time course of these single fibre EPSPs by assuming a restricted input location of synaptic input, despite obtaining a good match.

Figure 7 summarizes the effects of NBQX ejection on the peak amplitudes, rise times and half-widths of the single Ia fibre EPSPs examined in the present study. In each plot, straight lines representing no change and a reduction or increase of 50% of control values have been plotted for reference. Sequential averages of control EPSPs were used

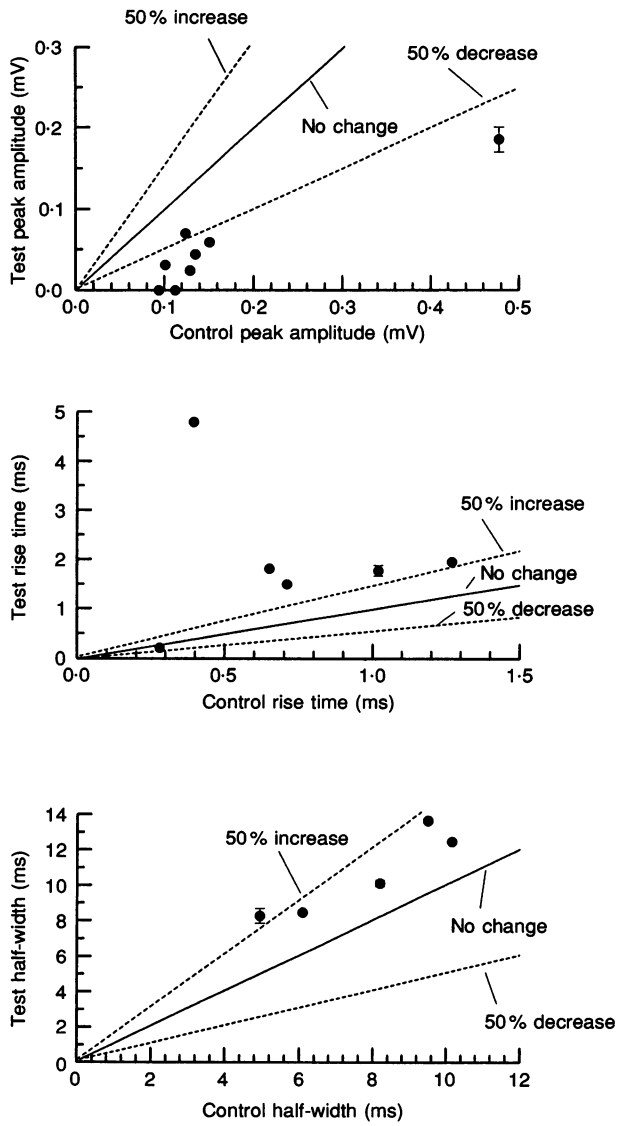


**Figure 7. Summary of the effect of local NBQX ejection on the peak amplitudes, rise times and half-widths of single Ia fibre EPSPs**

Control values of peak amplitude (*A*), rise time (*B*) and half-width (*C*) are plotted for each EPSP against the respective test values following local ejection of NBQX. Reference lines indicating no change and a 50% increase and 50% decrease compared with control values are plotted in *A*, *B* and *C*. The difference between sequential control average values is plotted as a vertical bar for each point to provide an indication of the reproducibility in these measurements. In nearly all cases the size of the plotted point is much greater than the amount of variation between successive measurements.

to determine the repeatability and accuracy of the parameters for each EPSP, in order to assess the changes in these parameters following NBQX ejection. This range is indicated as a vertical bar centred on each plotted data point. In most cases, the size of the plotted dot greatly exceeds this range. Figure 7*A* illustrates the considerable reduction in peak amplitude of all EPSPs studied, with a complete block for two EPSPs. On average, EPSPs were reduced in peak amplitude by 73% ($n = 8$) of control peak amplitude (average control repeatabilty within 2%). Figure 7*B* illustrates that there was generally a marked increase in the rise time of single fibre EPSPs associated with a decrease in amplitude (with the exception of one EPSP in which there was no significant change, also illustrated in Fig. 2*C*). On average, there was a 269% increase in the rise time ($n = 6$, average control repeatability within 9%). The average increase in half-width (Fig. 7*C*) for single fibre EPSPs was 37% ($n = 5$, average control repeatability within 9%). (Numbers of measurements of amplitude, rise time and half-width in *A*, *B* and *C* are different because of complete block and polysynaptic contamination of EPSP decay precluding time course measurements for several EPSPs, e.g. see Fig. 2.)

## DISCUSSION

Prior to the present experiments, previous intracellular studies have not been able to demonstrate a complete pharmacological block of the group Ia fibre EPSP in cat spinal motoneurones *in vivo* (although we have demonstrated complete block of the group I EPSP evoked in dorsal spinocerebellar tract neurones using central canal perfusion of kynurenate; Walmsley & Nicol, 1991*a*). The study by Flatman *et al.* (1987) used the antagonists GAMS and PDA to demonstrate a reduction of the composite group Ia EPSP. In the present study, the highly potent AMPA/kainate antagonist NBQX (Honoré *et al.* 1988; Sheardown, Nielson, Hansen, Jacobsen & Honoré, 1990; Watkins *et al.* 1990) has been used in conjunction with single group Ia fibre EPSPs to demonstrate a complete block of the Ia EPSP in cat spinal motoneurones. The AMPA/kainate antagonist NBQX was selected because it is considerably more potent than the antagonist CNQX (Sheardown *et al.* 1990). However, as in all previous experiments using local ejection of pharmacological agents, the concentration and therefore selectivity of the antagonist NBQX at the synaptic contacts was unknown in the present experiments. Although a potential lack of selectivity of the antagonist was not critical to the primary aim of the present study, the possible contribution of a slow time course (e.g. NMDA receptor-mediated) synaptic current needs to be considered. Jahr & Yoshioka (1986) used an *in vitro* preparation of the rat spinal cord to study the effect of known concentrations of excitatory amino acid receptor antagonists on Ia EPSPs evoked in motoneurones. Superfusion of 30–100 $\mu$M of the NMDA receptor antagonist APV did not affect the monosynaptic component of the EPSP, but did suppress later polysynaptic components. Most significantly, in the cat spinal cord *in vivo*, the time course of the synaptic current underlying single Ia fibre EPSPs has been directly measured in single-electrode voltage clamp experiments by Finkel & Redman (1983). These results demonstrated that the Ia synaptic current is extremely brief, with a time to peak of less than 0·2 ms and a simple exponential decay with a time constant of 0·3–0·4 ms. Furthermore, depolarization and reversal of the membrane potential to positive potentials did not reveal any slow underlying current, e.g. an NMDA receptor-mediated synaptic current which may have been blocked by $Mg^{2+}$ at more negative membrane potentials (Finkel & Redman, 1983). In the present experiments, the two single fibre EPSPs exhibiting the briefest rise times were completely blocked by NBQX ejection. Analysis of one of these EPSPs at reduced amplitude (between the control amplitude and complete block) did not reveal any slowing of the rise time compared to the control EPSP. Taken together, the available evidence therefore indicates that the synaptic current underlying single fibre Ia EPSPs is extremely brief, and is most probably generated by AMPA/kainate receptors.

The primary aim of the present experiments was to investigate the spatial distribution of active synapses over the motoneurone dendritic tree, arising from a single group Ia fibre. Previous studies have used the time course of the single group Ia fibre EPSP in conjunction with an electrotonic cable model of the motoneurone to indicate an electrotonic location of the synaptic contacts arising from the afferent fibre (Redman, 1971; Jack & Rall *et al.* 1967, 1992; Iansek & Redman, 1973*b*). These studies have generally assumed that the input is spatially restricted over the dendritic tree. Furthermore, a good match of the model transient to the time course of the EPSP has been taken as supporting evidence for a lack of spatial spread. However, in a subsequent modelling study (Walmsley & Stuklis, 1989) it has been demonstrated that it is generally not possible to use the time course of the synaptic potential in conjunction with a neuronal cable model to detect spatial dispersion of the synaptic input, even for extreme cases of spread of the synaptic input over the entire dendritic tree. A very close match can usually be obtained between the time course of the voltage transient generated by a distributed input and the voltage transient generated by an input at a single location (Walmsley & Stuklis, 1989).

Anatomical experiments have revealed that the putative synaptic contacts arising from a single Ia fibre are generally distributed over the dendritic trees of motoneurones (Brown & Fyffe, 1978; Burke *et al.* 1979; Glenn *et al.* 1982). However, it is not known whether all or only a small fraction of these synaptic contacts are active, i.e. release neurotransmitter. In fact, quantal analysis of

single group Ia fibre EPSPs, and experiments on $Ca^{2+}$ facilitation of transmission at this connection, indicates that transmitter release probability may be low (or zero) for many Ia synaptic contacts (Redman & Walmsley, 1983; Redman, 1990; Walmsley & Nicol, 1991*b*). The possibility exists, therefore, that although there may be a widespread anatomical distribution of synaptic contacts arising from a single Ia fibre, only a few of these contacts contribute significantly to the Ia EPSP. The present experiments have addressed this issue functionally by examining the progressive spatial postsynaptic block of active synapses by ejection of NBQX from an extracellular electrode in close proximity to the intracellular recording electrode. This technique produces the highest antagonist concentration closest to the recording site, resulting in a greater reduction in the amplitude of the most proximal active synapses (which contribute the briefest time course components to the EPSP). The results of these experiments reveal that, for the single Ia fibre EPSPs examined, there is a considerable slowing in the time course (in particular of the rising phase) of the EPSP during block by NBQX. The time course of the EPSP would not be expected to change if the active synapses contributing to the EPSP were at a restricted electrotonic location, and the most plausible explanation for this observation is that there is a considerable spatial spread in the distribution of active synapses arising from the single Ia afferent fibres and contacting the motoneurone. Because of the technical difficulties associated with these experiments, it was only possible to examine a limited number of single Ia afferent fibre connections. However, it is clear from the present results that it cannot be assumed that there is a spatially restricted distribution of active synapses arising from a single Ia afferent fibre. The results of the present study provide direct experimental support for our previous modelling study (Walmsley & Stuklis, 1989) which indicates that, in general, spatial dispersion of synaptic input cannot be detected using the time course of synaptic potentials in conjunction with an electrotonic neuronal cable model.

## REFERENCES


Brown, A. G. & Fyffe, R. E. W. (1978). The morphology of group Ia afferent fibre collaterals in the spinal cord of the cat. *Journal of Physiology* **274**, 111–127.

Burke, R. E., Walmsley, B. & Hodgson, J. A. (1979). HRP anatomy of group Ia afferent contacts on alpha motoneurones. *Brain Research* **160**, 347–352.

Davies, J. & Watkins, J. C. (1983). Role of excitatory amino acid receptors in mono- and polysynaptic excitation in the cat spinal cord. *Experimental Brain Research* **49**, 280–290.

Davies, J. & Watkins, J. C. (1985). Depressant action of D-glutamylaminomethyl sulfonate (GAMS) on amino acid induced and synaptic excitation in the cat spinal cord. *Brain Research* **327**, 113–120.

Finkel, A. S. & Redman, S. J. (1983). The synaptic current evoked in cat spinal motoneurones by impulses in single group Ia axons. *Journal of Physiology* **342**, 615–632.

Flatman, J. A., Durand, J., Engberg, I. & Lambert, J. D. C. (1987). Blocking the monosynaptic EPSP in spinal cord motoneurones with inhibitors of amino-acid excitation. In *Excitatory Amino Acid Transmission*, pp. 285–292. Alan R. Liss New York.

Glenn, L. L., Burke, R. E., Fleshman, J. W. & Lev-Tov, A. (1982). Estimate of electrotonic distance of group Ia contacts on cat alpha-motoneurons. *Society of Neuroscience Abstracts* **8**, 995.

Honoré, T., Davies, S. N., Drejer, J., Fletcher, E. J., Jacobsen, P., Lodge, D. & Nielsen, F. E. (1988). Quinoxalinediones: potent competitive non-NMDA glutamate receptor antagonists. *Science* **241**,701–703.

Iansek, R. & Redman, S. J. (1973*a*). An analysis of the cable properties of spinal motoneurones using a brief intracellular current pulse. *Journal of Physiology* **234**, 613–636.

Iansek, R. & Redman, S. J. (1973*b*). The amplitude, time course and charge of unitary excitatory post-synaptic potentials evoked in spinal motoneurones dendrites. *Journal of Physiology* **234**, 665–688.

Jack, J. J. B., Miller, S., Porter, R. & Redman, S. J. (1971). The time course of minimal excitatory post-synaptic potentials evoked in spinal motoneurones by group Ia afferent fibres. *Journal of Physiology* **215**, 353–380.

Jack, J. J. B. & Redman, S. J. (1971). An electrical description of the motoneurone and its application to the analysis of synaptic potentials. *Journal of Physiology* **215**, 321–352.

Jahr, C. E. & Yoshioka, K. (1986). Ia afferent excitation of motoneurones in the *in vitro* new-born rat spinal cord is selectively antagonized by kynurenate. *Journal of Physiology* **370**, 515–530.

Rall, W., Burke, R. E., Holmes, W. R., Jack, J. J. B., Redman, S. J. & Segev, I. (1992). Matching dendritic neuron models to experimental data. *Physiological Reviews* **72**, S159–186.

Rall, W., Burke, R. E., Smith, T. G., Nelson, P. G. & Frank, K. (1967). Dendritic location of synapses and possible mechanisms for the monosynaptic EPSP in motoneurons. *Journal of Neurophysiology* **30**, 1169–1193.

Redman, S. J. (1990). Quantal analysis of synaptic potentials in neurones of the central nervous system. *Physiological Reviews* **70**, 165–198.

Redman, S. J. & Walmsley, B. (1983). Amplitude fluctuations in synaptic potential evoked in cat spinal motoneurones at identified group Ia synapses. *Journal of Physiology* **343**, 135–145.

Sheardown, M. J., Nielsen, E. O., Hansen, A. J., Jacobsen, P. & Honoré, T. (1990). 2,3-Dihydroxy-6-nitro-7-sulfamoyl-benzo(F)quinoxaline: a neuroprotectant for cerebral ischemia. *Science* **247**, 571–574.

Tracey, D. J. & Walmsley, B. (1984). Synaptic input from identified muscle afferents to neurones of the dorsal spinocerebellar tract in the cat. *Journal of Physiology* **350**, 599–614.

Walmsley, B. (1992). Quantal analysis of synaptic transmission. In *Electrophysiology: A Practical Approach*, ed. Willis, D. I. Oxford University Press, Oxford, UK.

Walmsley, B. & Nicol, M. J. (1991*a*). The effects of $Ca^{2+}$, $Mg^{2+}$ and kynurenate on primary afferent synaptic potentials evoked in cat spinal cord neurones *in vivo*. *Journal of Physiology* **433**, 409–420.

Walmsley, B. & Nicol, M. J. (1991*b*). Calcium facilitation of group Ia EPSPs evoked in cat spinal motoneurones in vivo. *Neuroscience Letters* **126**, 184–186.

WALMSLEY, B. & STUKLIS, R. (1989). Effects of spatial and temporal dispersion of synaptic input on the time course of synaptic potentials. *Journal of Neurophysiology* **61**, 681–687.

WATKINS, J. C., KROGSGAARD-LARSEN, P. & HONORÉ, T. (1990). Structure–activity relationships in the development of excitatory amino-acid receptor agonists and competitive antagonists. *Trends in Pharmacological Sciences* **11**, 25–33.

**Acknowledgements**

We are very grateful to Drs Honoré and Sheardown of Novo-Nordisk (Copenhagen) for their generous gift of NBQX, and to the National Health and Medical Research Council of Australia for financial support for this project.

*Received 31 August 1993; accepted 13 May 1994.*